Search For Large Extra Dimensions in $p\bar{p}$ collider at $\sqrt{s} = 1.96$ TeV

Piyali Banerjee
Universite de Montreal

April 16, 2009

Plan of the talk I

- Theory of Large Extra Dimensions (LED)
- Tevatron Accelerator
- DØ Detector
- Data Analysis
- Efficiencies
- Background Estimation
- Monte Carlo Signal Generation
- Systematics
- Limit Setting
- Result

Theory Of LED I

- Standard Model (SM) based on $SU(3)_C \times SU(2)_L \times U(1)_Y$ gauge symmetry.
- Describes interaction of bosons and fermions.
- Gravity is not included

The Hierarchy and naturalness problem

- **electroweak scale: ~ 100 GeV**
  - M_W = 80 GeV, M_Z = 91 GeV, vev (H) = 246 GeV
- **Planck scale:** E_{Pl} $(\hbar c^5/G)^{1/2}$ 1.22 10^{19} GeV = length 1.6 10^{-32} mm
  - energy at which quantum effects of gravity become important

Why are the two scales so different ???

- **Radiative corrections to Higgs mass diverge in the SM !**

For Λ = 10 TeV, $\rightarrow$ $\delta m_h^2 \sim$ | $-\frac{3}{8\pi^2}\lambda_t^2\Lambda^2 \sim (2\ \text{TeV})^2$ | $\frac{1}{16\pi^2}g^2\Lambda^2 \sim (700\ \text{GeV})^2$ | $\frac{1}{16\pi^2}\lambda^2\Lambda^2 \sim (500\ \text{GeV})^2$

- **fine tuning ??** higher order terms must cancel very precisely

Theory Of LED I

"TeV scale extra dimensional model → LED (Arkani-Hamed,Dimopoulos and Dvali)"

- large spatial compactified dimensions n to our normal 3+1 dimensional space-time universe
- 3+1 (3-brane) dimensions form a n+4 (bulk) dimensional universe.

- SM particles are pinned to this 3-brane while gravity via graviton can propagate into these additional n space dimensions

Theory Of LED II

- Gauss's Law gives; Planck scale M_s, observed Planck scale M_{Pl}, the size of the extra dimension R and number of extra dimensions n

$$[M_{Pl}]^2 \sim R^n \, [M_s]^{n+2} \tag{0.1}$$

- If R can be large compared to Planck length, M_s can be as low as TeV
- The fundamental Planck scale is now at TeV, **the hierarchy problem is avoided**
- If $M_s \sim 1$ TeV then R goes as $10^{(30/n)-19}$m, so $R \sim 10^{11}m$ for $n = 1$, $\sim 1mm$ for $n = 2$, $\sim 3nm$ for $n = 3$, $\sim 10fm$ for $n = 6$.

Theory Of LED III

- probe for LED must be through the graviton interactions.

$$\phi(x,y) = \sum_{k_1} \cdots \sum_{k_n} \phi^{(k)}(x) e^{i\vec{k}\cdot\vec{y}/R} \tag{0.2}$$

- A graviton in the extra dimensions is equivalent from the $3+1$ dimensional point of view to a tower of infinite number of Kaluza-Klein (KK) states with $mass = \frac{2\pi k}{R}, k = 0, 1, 2, ...\infty$.
- The coupling strength of each of the KK states is $\frac{1}{M_{Pl}}$.
- A large number of modes can be excited at energy O(M_s)

Signatures of LED in Collider Experiment I

The collider based limits on M_s come from two channels:

1. **direct graviton emission**
2. **virtual graviton emission**

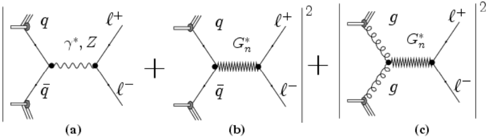

Gravity effects interfere with SM production amplitudes. Three terms contributing to production cross section: SM, interference, direct gravity effects:

$$\frac{d^2\sigma}{dMdcos\theta^*} = f_{SM} + \eta_G f_{int} + \eta_G^2 f_{KK} \qquad (0.3)$$

where f_{SM}, f_{int} and f_{KK} are functions of (M,cosθ^*).

Signatures of LED in Collider Experiment II

- Effect of ED parameterized by a single variable:

$$\eta_G = F/M_s^4 \tag{0.4}$$

- **GRW**: (Giudice, Rattazzi, Wells, $hep-ph/9811291$
  $F = 1$ (LO)
- **HLZ**: (Han, Lykken, Zhang, $hep-ph/9811350$
  $F = \log(M_s^2/s)$ for $n = 2$, $F = \frac{2}{n-2}$ for $n > 2$ (subleading n dependence)

$\Rightarrow$ different invariant mass and $cos\theta^*$ distribution as compared to pure SM process.

Experimental Status I

Collider

	Experiment	Channel	limits
direct graviton emission	L3	$e^+e^- \rightarrow \gamma(Z)G^k$	$M_d > 1.5 - 0.51$ TeV for $n = 2 - 8$
	all LEP	$e^+e^- \rightarrow \gamma(Z)G^k$	$M_d > 1.6 - 0.66$ TeV for $n = 2 - 6$
	CDF	$p\bar{p} \rightarrow jet + G^k$	$M_d > 0.55 - 0.6$ TeV for $n = 4 - 8$
	DØ	$p\bar{p} \rightarrow jet + G^k$	$M_d > 1 - 0.6$ TeV for $n = 2 - 7$
	DØ	$p\bar{p} \rightarrow \gamma(Z)G^k$	$M_d > 884 - 778$ GeV for $n = 2 - 8$
	CDF	$p\bar{p} \rightarrow \gamma(Z)G^k$	$M_d > 549, 581$ and 601 GeV for n=4, 6, and 8
virtual graviton emission	CDF	$p\bar{p} \rightarrow \mathbf{e}^+\mathbf{e}^-$ and $\gamma\gamma$	$M_s > 1.17 - 0.79$ TeV for $n = 3 - 7$
	DØ	$p\bar{p} \rightarrow \mathbf{e}^+\mathbf{e}^-$ and $\gamma\gamma$	$M_s > 1.0 - 1.4$ TeV for $n = 7 - 2$
	DØ	$p\bar{p} \rightarrow \mu^+\mu^-$	$M_s > 0.85 - 1.27$ TeV for $n = 7 - 2$

Non Collider I

Constraints on large ED

constraint	δ =2		δ =3	
	max R (mm)	min M_D (TeV)	max R (mm)	min M_D (TeV)
Gravitational force law	0.2	0.6		
SN1987A cooling by graviton emission	7 x 10^{-4}	10 30	9 x 10^{-7}	0.8 2.5
Diffuse cosmic ray background ($G^{(k)} \rightarrow \gamma\gamma$) other reheating scenarios decays after SN explosion	9 x 10^{-5}	25 167 450	2 x 10^{-7}	1.9 22 30
heating of neutron stars (trapped $G^{(k)}$ decaying)	8 x 10^{-6}	90 1700	3.5 x 10^{-8}	5 60

Tevatron Accelerator I

Tevatron Accelerator II

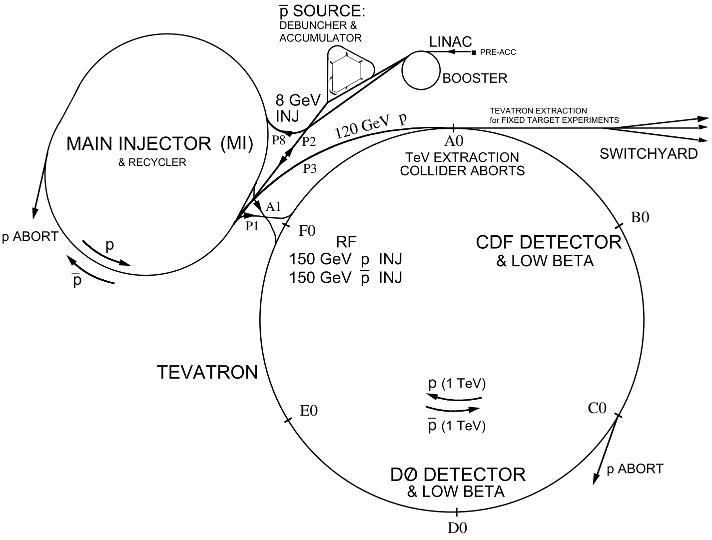

Figure: The general layout of the collider facility at Fermilab.

- The Fermilab Accelerator complex accelerates the proton and antiproton to energy of 980 GeV
- Collides at $\sqrt{s} = 1.96$ TeV at the two collision points located at CDF and DØ.
- Eight different acclerators (six circular and two linear)
- H^- ions are made from hydrogen atoms by addition of electrons.
- H^- ions are accelerated by Cockroft-Walton to 750 KeV.
- Linac, 150 m long accelerator raises energy of H^- to 400 MeV
- Enters booster
- Passes through carbon foil which strips of the electrons creating protons.

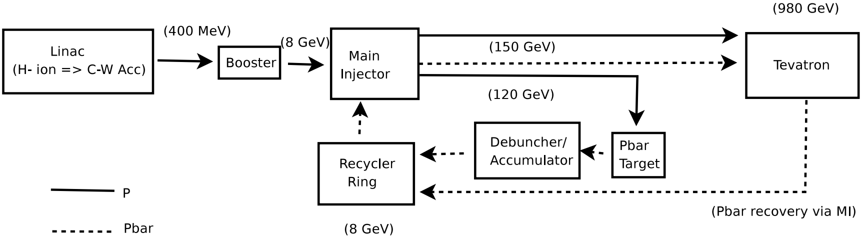

Figure: Schematic view of the collider facility at Fermilab.

Booster $\rightarrow$ 400 MeV to 8 GeV. Debuncher $\rightarrow$ large energy and narrow time spread into narrow energy and large time spread in 100 msec.

DØ Detector I

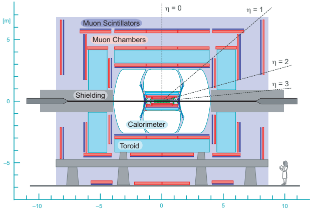

Figure: A view of the DØ Run II upgraded detector.

- Weighs 5500 tons, measures 13m(height) $\times$ 11m $\times$ 17m (length)
- The DØ uses right handed cylindrical coordinate system such that the direction of the protons is the positive z direction positive y direction points up.

DØ Detector II

- Transverse spread ∼ 30 microns; longitudinal spread ∼ 30 cm
- Luminosity monitor at $z = 140$ cm measures inelastic $p\bar{p}$ collisions

$$N = \sigma L \tag{0.5}$$

- 2.37 m long beryllium beam pipe and extends radially $37.6 - 38.1$ mm

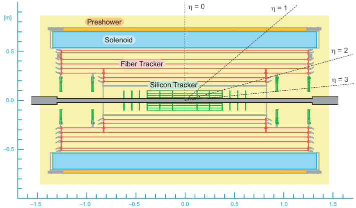

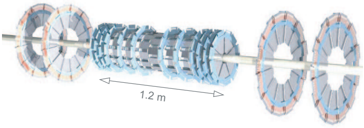

DØ Detector III

Primary interaction vertex, resolution $\sim$ 35 μm along z
Position resolution 15 μm in r-ϕ
Momentum resolution $\sim 5\%$ for $p_T \simeq 10$ GeV at $|\eta| = 0$
Silicon module $\Rightarrow$ "ladders", Barrels-$|z| = 6.2, 19, 31.8cm$
H-disks-$|z| = 100.4, 121cm$
F-disks-$|z| = 12.5, 25.3, 38.2, 43.1, 48.1, 53.1cm$
Secondary vertex resolution $\sim$ 40 μm in r-ϕ and $\sim$ 80 μm in r-z

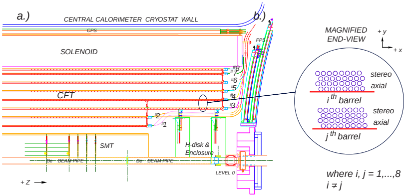

Scintillating fibers
8 concentric cylinders
(20 cm - 52 cm)
Eight doublet layers
2 axial and two stereo at ± 3
$|\eta| < 1.7$

Light from the fibers is converted to electrical pulse(Visible light photon Counters)

DØ Detector IV

Momentum resolution $\sim 8\%$ for $p_T \simeq 45$ GeV
Position resolution $\simeq 100\mu m$

DØ Detector V

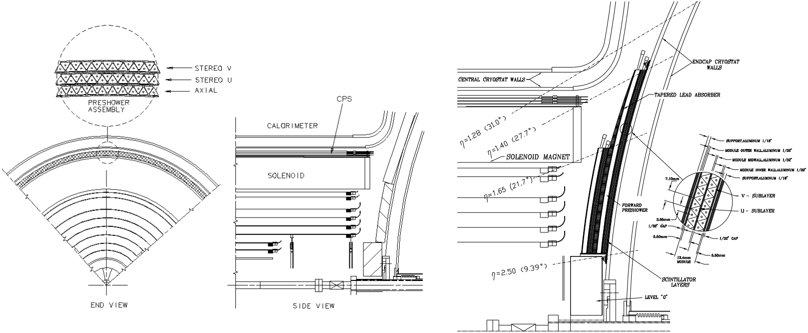

CPS covers $|\eta| < 1.3$ and extends radially (71.19 - 73.61) cm

FPS covers $1.5 < |\eta| < 2.5$, has mip and shower layers

Shower layer made of scintillating strips (axial + stereo $\pm 23^0$) for CPS

DØ Detector VI

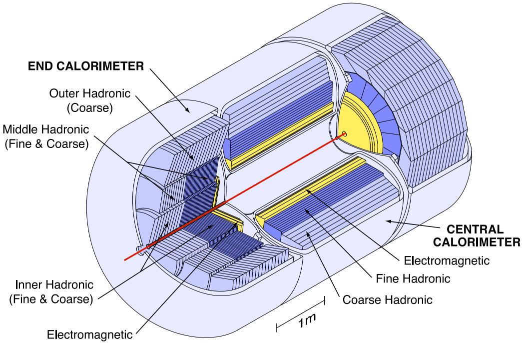

1) Energy measurements
2) Assists in identification
e,γ,jets,μ
sampling calorimeter
$Uranim/liquid - argon$
Uranium absorber
Liguid Ar as active medium

$1.4, 2, 6.8, 9.8 X_0$ thick in CC and $1.6, 2.6, 7.9, 9.3 X_0$ in EC for EM calorimeter
128.9 X_0 thick in CC, 373 X_0 thick in EC for Hadronic Calorimeter
0.76, 3.2, 3.3 λ in CC 0.95, 4.9, 3.6, 4, 4.1, 7 λ in EC

DØ Detector VII

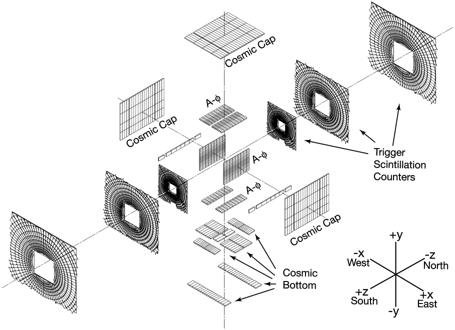

Proportional Drift tubes(CC)
Mini drift tubes (EC)
CMS covers $|\eta| \lesssim 1.0$
FMS covers $|\eta| \approx 2.0$

The Scintillators are used for triggering
The wire chambers are used for coordinate measurement and triggering

DØ Detector VIII

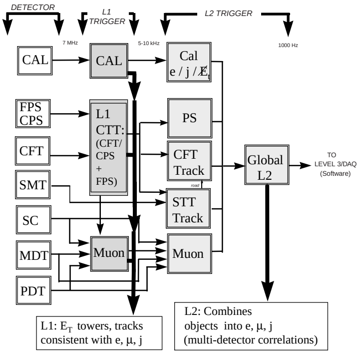

Example of 2 calorimeter based triggers

v13: **E3_2L20**

CEM(1,9)CEM(2,3), L2CALEM(1,15), ELE_NLV(2,20)

v14: **E3_SHT25**

CEM(1,12), L2CALEM(1,11,0.2), ELE_NLV_SHT(1,25)

L1 Trigger terms
CEM(1, 9)CEM(2, 3) : one EM trigger tower with $E_T > 9$ GeV, and another EM trigger tower with $E_T > 3$ GeV
CEM(1, 12) : one EM trigger tower with $E_T > 12$ GeV
L2 Trigger terms
L2CALEM(1,15) : one standard L2 EM cluster with a threshold $E_T > 15$ GeV
L2CALEM(1,11,0.2) : one single EM cluster with isolation < 0.2 and $E_T >= 11$GeV
L3 trigger terms
ELE_NLV(2,20) : two electrons with $E_T > 20$ GeV satisfying loose requirements and with $|\eta| < 3.6$
ELE_NLV_SHT(1,25) : one electron with $|\eta| < 3.6$ and $E_T > 25$ GeV passing tight shower shape cuts

Data Analysis I

Since RunII, $3\,fb^{-1}$ of data to tape. This analysis is based on $1.1 fb^{-1}$ of data (October 2002 and February 2006). 2EM candidates as final state (photons and electrons)

Cuts Applied: (satisfied by both EM candidates)

- Remove all events calorimeter bad runs and luminosity blocks.
- Passes OR of single and di-EM Triggers
- $|\eta| < 1.1$ (Central Calorimeter, CC) and $1.5 < |\eta| < 2.4$ (EndCap Calorimeter, EC)
- p_T of the EM candidate should be above 25 GeV
- Fraction of energy in the electromagnetic calorimeter $f_{EM} > 0.97$ for CC and $f_{EM} > 0.97$ for EC.
- Fraction of energy in the isolation cone $\frac{E_{Tot}(0.4) - E_{EM}(0.2)}{E_{EM}(0.2)} = f_{iso} < 0.07$

Data Analysis II

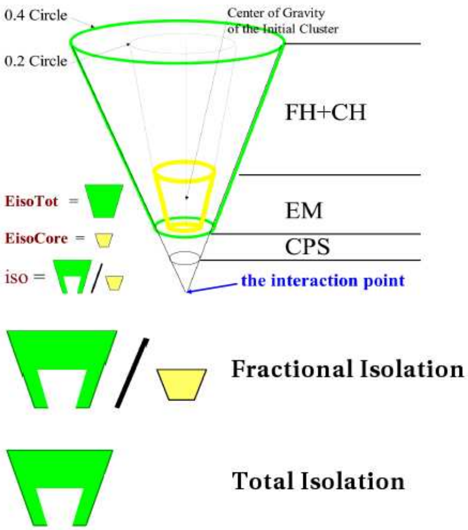

Data Analysis III

- Sum of transverse momenta of tracks in a hollow cone p_{iso} within $0.05 < \Delta R < 0.4$, with respect to the direction of the EM candidate should be $< 2\,GeV$ in CC, and $< 1\,GeV$ in EC, where $\Delta R = \sqrt{(\Delta\eta^2 + \Delta\phi^2)}$
- Electromagentic shower shape profile be consistent with that of an electron or photon using a χ^2 test cut with different shower shape variables should be
  - 7×7 H-matrix $\chi^2 < 12$ in CC.
  - 8×8 H-matrix $\chi^2 < 20$ in EC.
- Variables constructed with Forward Pre Shower
  I) Energy of the highest energy cluster from all the matched FPS clusters in the shower layer $E_{shower} < 0.12$ GeV
  II) Number of matched FPS clusters in the shower layer must be $<= 4$.

Data Analysis IV

" Observed number of Events (N_{Obs})"

Efficiency Determination: I

The same dataset is used to determine the di-EM detection efficiency. Efficiencies needed

(I) Trigger efficiency for various trigger versions.

(II) Efficiency due to shower shape (H-matrix χ^2) cuts.

(III) Combined efficiency due to EM-fraction (f_{EM}) and isolation (f_{iso} and p_{iso}) cuts.

▷ Determined efficiency as a function of p_T and η

▷ Folded these efficiencies into MonteCarlo

Efficiency Determination: II

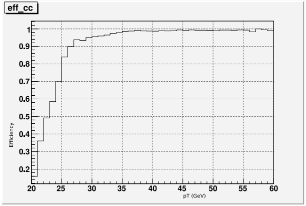

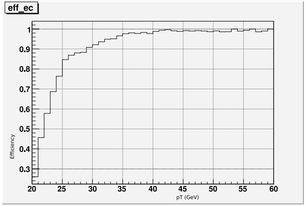

Figure: pT turn of "OR" of all the single and di-EM triggers from all the four different trigger versions in **Left:** CC **Right:** EC

Efficiency Determination: III

For a given set of OR-ing of triggers from a trigger version the efficiency is given by

$$\epsilon_{tot}^{v12} = 1 - (1 - \epsilon(p_{T1})) * (1 - \epsilon(p_{T2})) \tag{0.6}$$

Here ϵ_{tot}^{v12} is the total efficiency for all the triggers from version 12. Combined efficiency for the event to pass OR of single and di-EM trigger is

$$\begin{aligned} P &= \epsilon(p_{T1}) + (1 - \epsilon(p_{T1})) * \epsilon(p_{T2}) \\ &\quad + (1 - \epsilon(p_{T1})) * (1 - \epsilon(p_{T2})) * D(p_{T1}) * D(p_{T2}) \end{aligned} \tag{0.7}$$

where $D(p_{T1})$ and $D(p_{T2})$ be the efficiencies to fire di-EM trigger with momentum p_{T1} and p_{T2} by the two EM candiadates if already failed single-EM trigger.

Efficiency Determination: IV

$$E_{total} = \frac{\epsilon_{tot}^{v8-v11}\mathcal{L}_{v8-v11} + \epsilon_{tot}^{v12}\mathcal{L}_{v12} + \epsilon_{tot}^{v13}\mathcal{L}_{v13} + \epsilon_{tot}^{v14}\mathcal{L}_{v14}}{\mathcal{L}_{total}} \quad (0.8)$$

where $\mathcal{L}_{v8-v11}$, $\mathcal{L}_{v12}$, $\mathcal{L}_{v13}$, $\mathcal{L}_{v14}$ are the highest recorded luminosity from each trigger version.

Background Estimation I

Dominant Backgrounds:

1. **SM processes of Z/Drell-Yan and $\gamma\gamma$**
2. **Instrumental fakes due to dijets and $\gamma + jets$ (QCD)**

QCD Background Estimation:

▷ Estimated from data. ▷ Cuts Applied

- $pT > 25$ GeV (for both EM candidates)
- Either one of the di-EM candidates must satisfy
  $Hmx7 > 20$ (CC)
  $Hmx8 > 20$ (EC),

→ **"gives us the shape of QCD (h_{QCD})"**

Background Estimation II

Physics Background:

- ▷ Physics background is obtained using PYTHIA
- ▷ Used constant k-factor for both Z/Drell-Yan and $\gamma\gamma$ production

Process	Mass Window (GeV)	LO Cross Section (pb)	Number of Event generated
DY	60-130	178	264750
	130-250	1.3	27500
	250-500	0.11	27000
	$>$500	0.0045	25500
$\gamma\gamma$	50-130	42.7	50500
	130-250	3.1	51500
	250-500	0.49	26750
	$>$500	0.034	25500

Table: List of DY and $\gamma\gamma$ MonteCarlo samples used in this analysis

Background Estimation III

Both the ee and $\gamma\gamma$ must satisfy

- must either lie in CC or EC
- $pT > 25$ GeV
- $f_{EM} > 0.97$
- $f_{iso} < 0.07$
- $p_{iso} < 2\,GeV$ in CC, and $< 1\,GeV$ in EC
- $Hmx7 < 12$ (CC) and $Hmx8 < 20$ (EC)

$\rightarrow$ **"gives us the shape of SM (h_{SM})"**

To get actual contributions consider the mass interval [60 - 140 GeV] $\rightarrow$ no LED signal

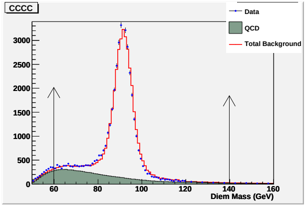

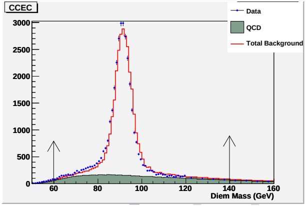

Background Estimation IV

$$N_{Obs} = A * h_{SM} + B * h_{QCD} \tag{0.9}$$

A and B determined by fit using χ^2 *minimization*

- Normalized with respect to luminosity for all the 4 mass range
- Normalize both SM and QCD distribution to its Integral in the mass $[60 - 140]$ GeV
- Scale both SM and QCD distribution to total number of observed events in mass $[60 - 140]$ GeV
- extrapolation of background using A and B for $M > 240GeV \Rightarrow$ expected background events
- gives us N_{SM} and N_{QCD}

Background Estimation V

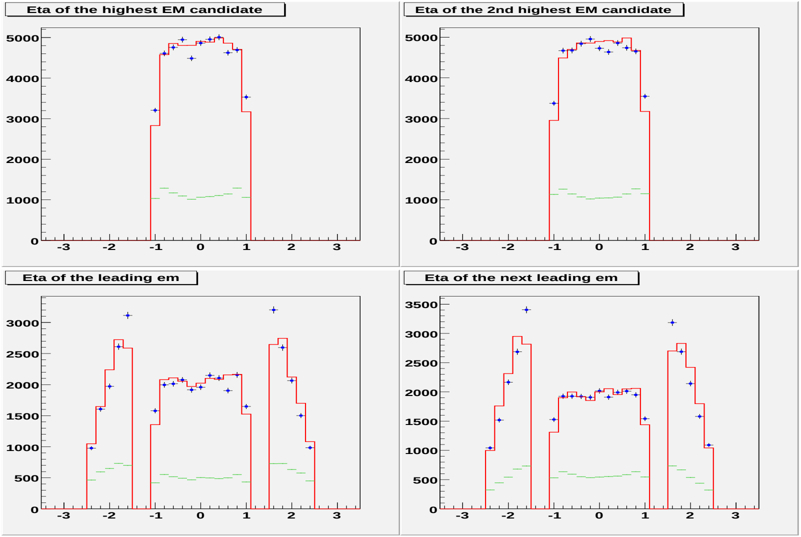

Background Estimation VI

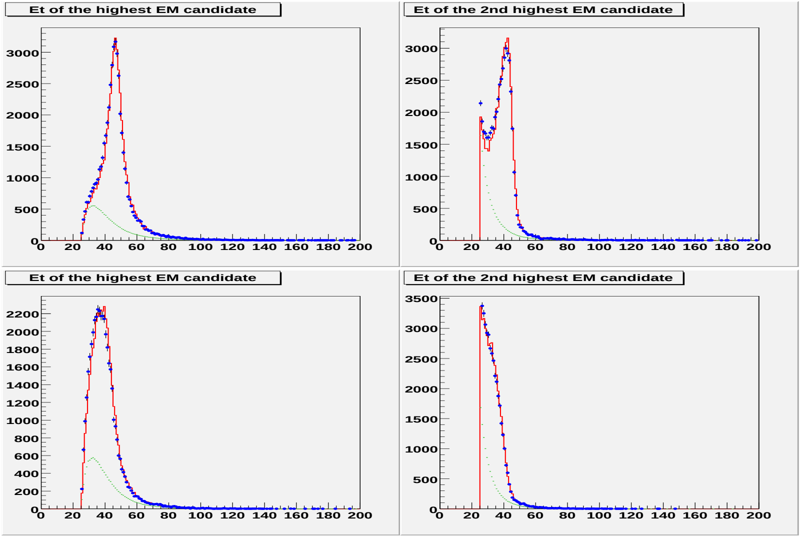

Background Estimation VII

Table: Number of events observed and expected from SM and multijet background in different mass windows for CC-CC events. Also the individual contributions to the total background events from multijet, $\mathbf{e^+e^-}$ and $\gamma\gamma$ are shown separately.

Mass (GeV)	Data N	Total Background $N_b \pm N_b^{\text{sys}}$	Multijet $N_{\text{MJ}} \pm N_{\text{MJ}}^{\text{sys}}$	$\mathbf{e^+e^-}$ $N_{\mathbf{e^+e^-}}$	$\gamma\gamma$ $N_{\gamma\gamma}$
240–290	61	67 ± 8	22 ± 3.1	30	15
290–340	30	28 ± 4	7 ± 1.1	14	7
340–400	21	15 ± 2	3 ± 0.5	7	5
400–500	9	9 ± 1.2	1.4 ± 0.3	5	3
500–600	1	4 ± 1.16	0.14 ± 0.09	2.4	1.1
600–1000	2	1.3 ± 0.07	0.11 ± 0.06	0.67	0.53

Background Estimation VIII

Table: Number of events observed and expected from SM and multijet background in different mass windows for CC-EC events. Also the individual contributions to the total background events from multijet, $\mathbf{e^+e^-}$ and $\gamma\gamma$ are shown separately.

Mass (GeV)	Data N	Total Background $N_b \pm N_b^{\mathsf{sys}}$	Multijet $N_{\mathsf{MJ}} \pm N_{\mathsf{MJ}}^{\mathsf{sys}}$	$\mathbf{e^+e^-}$ $N_{\mathbf{e^+e^-}}$	$\gamma\gamma$ $N_{\gamma\gamma}$
240–290	144	171 ± 34	115 ± 34	34	30
290–340	52	55 ± 11	35 ± 11	12	8
340–400	21	23 ± 5	12 ± 4	7	4
400–500	12	9 ± 2	4 ± 1.5	3.3	1.2
500–600	2	2 ± 0.43	0.59 ± 0.23	0.73	0.18
600–1000	0	0.36 ± 0.07	0.03 ± 0.04	0.24	0.008

LED Signal Generation: I

- Used standalone MonteCarlo generator
- Calculates only tree level cross section
- Detector effects and ISR is taken into account:
  ▷Generated SM and SM+LED cross-sections(σ) separately for both channels for different a given M_s
  ▷Generated for all cosθ^* bin for invariant mass $[0, 1000]$ GeV
  ▷**Ratio** of these two σ gives the enhancement of the SM σ due to LED
  ▷Folded it as **weight** into (DØ detector simulated) full chain SM(ee and $\gamma\gamma$) MonteCarlo generated with PYTHIA
  ▷ repeated for various M_s and n.

LED Signal Generation: II

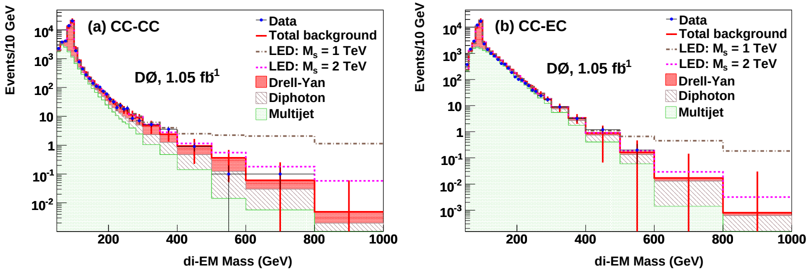

Figure: The di-EM invariant mass distributions for CC-CC (a) and CC-EC (b) events.

LED Signal Generation: III

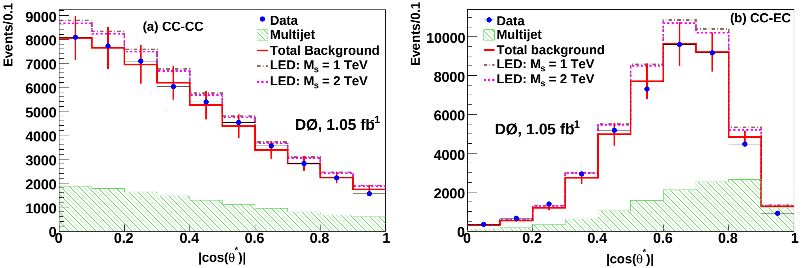

Figure: The distributions of the center-of-mass scattering angle $\cos\theta^*$ of the two final state EM candidates in CC-CC (a) and CC-EC (b) events.

Sources of Sytematic Uncertainties: I

		CC-CC	CC-EC
Signal only			
	Acceptance	1–19	1.5–12
	Luminosity	4	4
Signal and background			
	Trigger + EM selection	6	5
	Energy scale	5–13	0.3–3.5
	Energy resolution	0.3–1.7	0.2–3.5
	NLO k-factor	3–10	3–10
	k-factor mass dependence	5	5
	PDF	5.5–9	5.5–9
Background only			
	Multijet	13	30

Limit Setting: I

$\rightarrow$ Observed events were compared with LED+SM+QCD for invariant mass > 240 GeV and $\forall$ cosθ^* for various M_s
$\rightarrow$ Repeated for various n.
For a given M_s the expected number of events in the k^{th} mass bin and l^{th} cosθ^* bin is

$$N^{kl}(M_s) = B^{kl} + N^{kl}_{LED}(M_s) \tag{0.10}$$

$\rightarrow$ B^{kl} is the combined expected number of background events due to SM physics and fake.
$\rightarrow$ $N^{kl}_{LED}(M_s)$ is the expected signal events due to LED
The **posterior probability** density for a M_s given N^{kl}_{obs} in the k^{th} mass bin and l^{th} cosθ^* bin is

Limit Setting: II

$$P(M_s|Data) = \frac{1}{A}\int dB^{kl} dN^{kl}_{LED} \prod_{k=0}^{n}\prod_{l=0}^{m}\left[e^{-N^{kl}_{M_s}} \frac{N^{kl\ N^{kl}_{obs}}_{M_s}}{N^{kl}_{obs}!}\right] \times P(M_s) \times P(N^{kl}_{LED}(M_s) + B^{kl}) \quad (0.11)$$

$\rightarrow$ Gaussian prior probability distribution $P(N^{kl}_{LED}(M_s) + B^{kl})$
$\rightarrow$ Mean $N^{kl}_{LED}(M_s) + B^{kl}$ and sigma from errors due to uncertainties
$\rightarrow$ $1/M_s^4$ prior probabilty distribution for $P(M_s)$
$\rightarrow$ No peak in $P(M_s|Data)$ other then at $1/M_s^4 = 0$
$\rightarrow$ lower limit, at 95% confidence level, on M_s using a semi-frequentist approach $\rightarrow$ log-likelihood ratio (LLR).

Limit Setting: III

$$LLR(\vec{s},\vec{b},\vec{d}) = -2\ln(Q) = \sum_{i=0}^{N_c}\sum_{j=0}^{N_{bins}} s_{ij} - d_{ij}\ln(1+\frac{s_{ij}}{b_{ij}}) \quad (0.12)$$

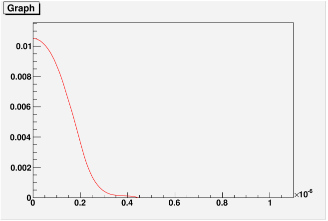

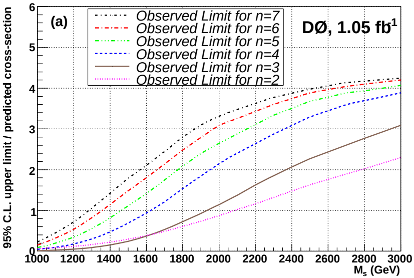

Limit Setting: IV

$\eta_G = F/M_s^4$, $F = 1$ for $n_d = 4$ in HLZ and GRW.
In GRW the observed limit for M_s is 1.62 TeV.
The limit on η_G is $<$ 0.145 TeV^{-4}.

Final Limits: I

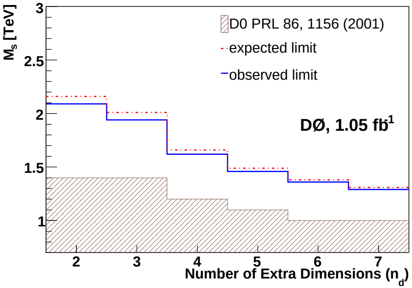

Figure: Observed and expected limits on the effective Planck scal e, M_s, in the di-EM channel along with previously published limits in di-EM channel.

"Phys. Rev. Lett. 102, 051601 (2009),arXiv.org:0809.2813 "

Final Limits: II

- N. Arkani-Hamed, S. Dimopoulos, and G. Dvali, Phys. Lett. B **429**, 263 (1998); I. Antoniadis, N. Arkani-Hamed, S. Dimopoulos, and G. Dvali, Phys. Lett. B **436**, 257 (1998); N. Arkani-Hamed, S. Dimopoulos, and G. Dvali, Phys. Rev. D **59**, 086004 (1999); N. Arkani-Hamed, S. Dimopoulos, and J. March-Russell, Phys. Rev. D **63**, 064020 (2001).
- J. L. Hewett, Phys. Rev. Lett. **82**, 4765 (1999); K. Cheung, Phys. Lett. B **460**, 383 (1999); K. Cheung and G. Landsberg, Phys. Rev. D **62**, 076003 (2000); K. Cheung, Phys. Rev. D **61**, 015005 (2000); O. J. P. Eboli et al, Phys. Rev. D **61**, 094007 (2000).
- G. Giudice, R. Rattazzi, and J. Wells, Nucl. Phys. **B544**, 3 (1999), and revised version arXiv:hep-ph/9811291.

Final Limits: III

- T. Han, J. Lykken, and R. Zhang, Phys. Rev. D **59**, 105006 (1999), and revised version arXiv:hep-ph/9811350.
- V. M. Abazov *et al.* (D0 Collaboration), Nucl. Instrum. Methods in Phys. Res. A **565**, 463 (2006).
- B. Abbott *et al.* (D0 Collaboration), Phys. Rev. Lett. **86**, 1156 (2001).
- D. Gerdes *et al.*, Phys. Rev. D **73**, 112008 (2006).
- B. Abbott *et al.* (D0 Collaboration), Phys. Rev. Lett. **95**, 161602 (2005).
- B. Abbott *et al.* (D0 Collaboration), Phys. Rev. Lett. **101**, 011601 (2008); T. Aaltonen *et al.* (CDF Collaboration), Phys. Rev. Lett. **101**, 181602 (2008).

Final Limits: IV

- B. Abbott *et al.* (D0 Collaboration), Phys. Rev. D **76**, 012003 (2007).
- T. Sjöstrand, S. Mrenna, and P. Skands, JHEP **0605**, 026 (2006); we used version 6.323.
- J. Pumplin *et al.*, JHEP **0207**, 012 (2002); D. Stump *et al.*, JHEP **0310**, 046 (2003).
- R. Brun and F. Carminati, CERN Program Library Long Writeup W5013, 1993 (unpublished).
- P. Mathews, V. Ravindran, K. Sridhar, and W. L. van Neerven, Nucl. Phys. **B713**, 333 (2005); R. Hamberg, W.L. van Neerven, and T. Matsuura, Nucl. Phys. **B359**, 343 (1991) [Erratum-ibid. **B644**, 403 (2002)].

Final Limits: V

- K. Cheung and G. Landsberg, Phys. Rev. D **62**, 076003 (2000).
- T. Junk, Nucl. Instrum. Methods. A **434**, 435 (1999); A. Read, "Modified Frequentist Analysis of Search Results(The CLs Method)",CERN 2000-005 (2000); W. Fisher, FERMILAB-TM-2386-E (2007).

Vote of Thanks: I

Prof N. K. Mondal, Dr A. Meyer, Dr J. Stark, Prof Y. Greshtien, Prof G. Landsberg, EB-012, Prof K Shridhar. Universite de Montreal, Prof Claude LeRoy, Prof Georges Azuelos for supporting me to complete this work.

Backup: I

$$N^{SM} = L \times (\sigma^{DY}_{NLO} \frac{N^{DY}_{[60-140GeV]}}{N^{DY}_{gen}} + \sigma^{\gamma\gamma}_{NLO} \times \frac{N^{\gamma\gamma}_{[60-140GeV]}}{N^{\gamma\gamma}_{gen}}) \quad (0.13)$$

where L is the integrated luminosity. We get $1047.35 pb^{-1}$ for L.

N^{DY}_{gen}	$\sigma^{DY}_{NLO}(pb)$	$N^{DY}_{[60-140GeV]}$	$N^{\gamma\gamma}_{gen}$	$N^{\gamma\gamma}_{[60-140GeV]}$	$\sigma^{\gamma\gamma}_{NLO}(pb)$	N^{data}	A
264750	178×1.34	37342	50500	666	42.7×1.34	45776	0.217

Assuming the same compactification radius R $\forall$ n, gravitational potential of m on unit mass in 4+n dimension is

$$\Phi(r_\perp, 0) = \Sigma_{k=-\infty}^{k=\infty} \frac{G_N^{4+n} \times m}{r_\perp^2 + \Sigma_i^n k^2 R_i^2} \tag{0.14}$$

$$\bigtriangledown^2 \Phi = -\frac{2^{n/2}}{\Gamma(n/2)} \times G_N^{3+n} \rho_M M \tag{0.15}$$

where G_N^{3+n} is the Newtons Gravitational constant in $3+n$ space dimansion and ρ_M is the mass density. Solving for Φ due to gravitaional action of m on unit mass in 3 flat space and n compa ctified space dimensions we get

$$\Phi = \frac{G_N^{3+n} \times m}{r_\perp^2 + \Sigma_i^n x_i^2} \tag{0.16}$$

where $x_i \simeq x_i + kR_i$, $\forall$ k. The scalar potential Φ then satisfies the periodic boundary condition

$\Phi(0) = \Phi(R) = \Phi(2R) = ...\Phi(kR)$

Hence we get,

$$\Phi(r_\perp, 0) = \Sigma_{k=-\infty}^{k=\infty} \frac{G_N^{3+n} \times m}{r_\perp^2 + \Sigma_i^n k^2 R_i^2} \tag{0.17}$$

For simplicity we assume that $R_i = R$, $\forall$ R.
Two cases arise out of the equation .I) $|r| << R$ and II) $|r| >> R$.
In caseI when m and the unit test mass will feel a $3+n$ dimensional gravitational potential and above equation reduces to

$$\Phi = \frac{mG_N^{3+n}}{r^{n+1}} \tag{0.18}$$

In case II when the masses are placed at the distance $|r| >> R$ from each other, the gravitational flux cannot penetrate extra dimensions and the potential is given by

$$\Phi = \frac{mG_N^{3+n}}{R^n r} \tag{0.19}$$

Since Fundamental Planck mass $M_{Plank}^{4+n} \sim 1/\sqrt{G_N^{4+n}}$ we get

$$\left[M_{Pl}^{4}\right]^{2} \sim R^{n}\left[M_{Pl}^{4+n}\right]^{n+2} \tag{0.20}$$

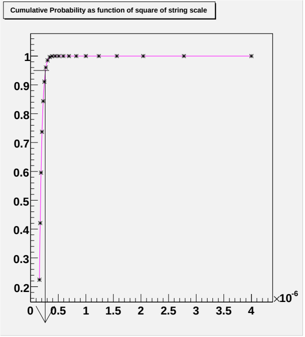

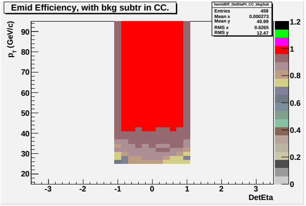
Emid Efficiency, with bkg subtr in CC.
Entries 459
Mean x 0.000273
Mean y 40.99
RMS x 0.6265
RMS y 12.47
p_T (GeV/c)
DetEta

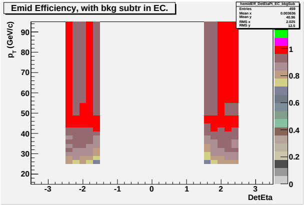
Emid Efficiency, with bkg subtr in EC.
Entries 459
Mean x 0.003636
Mean y 40.96
RMS x 2.025
RMS y 12.5
p_T (GeV/c)
DetEta

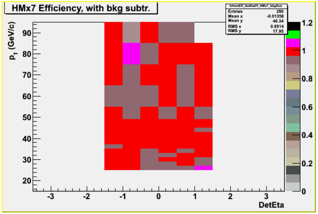
HMx7 Efficiency, with bkg subtr.
Entries 280
Mean x -0.01358
Mean y 46.34
RMS x 0.8514
RMS y 17.95
p_T (GeV/c)
DetEta

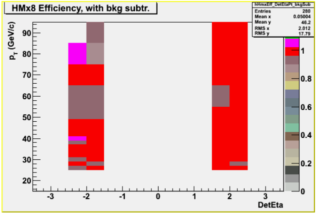
HMx8 Efficiency, with bkg subtr.
Entries 280
Mean x 0.05004
Mean y 46.2
RMS x 2.012
RMS y 17.79
p_T (GeV/c)
DetEta

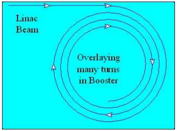

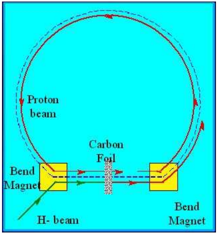

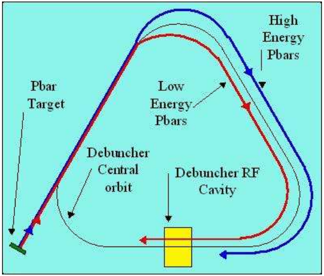

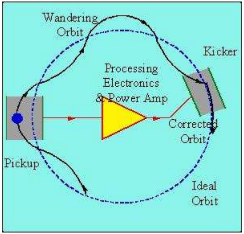

Pulse length in linac is 2.2 msec while for booster circumference is 2.2 msec long